ROTATION INVARIANT FEATURE EXTRACTION FOR WATERMARKING

M. Scagliola and P. Guccione
Dipartimento di Elettrotecnica ed Elettronica, Politecnico di Bari, Via E. Orabona 4, 70125 Bari, Italy

Keywords: Watermarking, Radon Transform, Rotation Invariant.

Abstract: Many watermarks for still images are robust against common signal processing techniques, mainly JPEG compression, noise adding and low-pass filtering, while they are sensitive to geometrical manipulations, that yield desynchronization errors.
In this paper robustness against some geometric transformations is achieved using a feature extraction method based on the Radon transform and whose aim is to identify an unique (and robust) feature from the image spectrum. The embedding, which exploits the extracted feature, is based on a multiplicative rule technique and is applied on a suitable subset of the image Fourier transform. The properties of the extracted feature allows to resynchronize the detector and the embedded watermark even if the image undergoes geometric manipulations (in particular rotations) as well as other processings, so that the correct watermark retrieving is guaranteed.
Experimental results, lead on many standard images, confirm the effectiveness of the feature extraction method and the robustness of the watermark against both processing and geometric transformations.

1 INTRODUCTION

Digital watermarking is a technique to hide an information, called the watermark, into a cover media. Watermark techniques play an important role in the copyright protection of multimedia such as images, sounds and video. In a blind watermarking context, the detector must be able to detect the mark on a received image that has undergone a certain number of unknown manipulations of an unknown entity, without owning any information about the original image.

While many watermarking methods perform well against the common signal processing techniques (mainly filtering, noise adding and compression), they lack robustness against geometric distortions, such as rotation, scaling, translation, cropping/shearing, projective transformation, (Licks and Jordan, 2005). This is justified by the different impact that these classes of distortions have on the embedded watermark; in fact, while the common signal processing techniques reduce the watermark energy, geometric distortions induce synchronization errors between the embedder and the detector.

Geometric attacks can be both unintentional and intentional; for example, an unintentional geometric attack occurs when a marked image is printed and scanned, as in the scanning process the image can be slightly rotated with respect to the sampling grid. On the other hand a geometric attacks can be performed intentionally by an attacker with the aim of impair the watermark detection, exploiting the weakness of the watermarking system.

Therefore achieving robustness against geometric transformations has become a widely studied topic in digital image watermarking.

Several strategies have been proposed for watermark detection after geometric distortions. A rough classification divides these schemes into template insertion, invariant domain based schemes and feature-based algorithms (Licks and Jordan, 2005). Templates are registration patterns which are inserted into the image in addition to the watermark, allowing the synchronization of the embedder and detector. This solution may reduce the image fidelity and the watermark capacity; moreover templates are susceptible to removal or estimation attacks (Licks and Jordan, 2005). The Fourier-Mellin domain is often used in watermarking since it is proved to be theoretically invariant to rotation, scaling and translations (RST) transformations. Thus, if the watermark is embed-

Scagliola M. and Guccione P. (2008).
ROTATION INVARIANT FEATURE EXTRACTION FOR WATERMARKING.
In *Proceedings of the International Conference on Signal Processing and Multimedia Applications*, pages 229-235
DOI: 10.5220/0001931502290235

ded into the Fourier-Mellin transform of an image, the robustness with respect to these geometrical transformations is provided (ÓRuanaidh and Pun, 1998), (Lin et al., 2001). Actually, as stated in (Lin et al., 2001), the Fourier-Mellin transform is considered an expensive solution to cope with RST attacks and the problem of inverting this map is a quite difficult task. Feature-based algorithms are founded on the capability to identify certain image features (edges, corners and so on) before and after an attack. A huge variety of features have been used in several methods to provide geometric robustness: for example Bas et al. use a corner detector to construct a triangular tessellation where the mark is embedded (Bas et al., 2000); in (Simitopoulos et al., 2002) two one-dimensional generalized Radon transforms are used; in (Xin et al., 2004) an expansion of the image based on the Pseudo-Zernike basis has been proposed with the properties of RST invariance.

In this paper we present a watermarking technique robust against rotation distortion and other common signal processing, which is based on the capability to extract a single invariant direction from the image spectrum, used just to synchronize the detector and the watermark. We start from the properties of the Fourier-Mellin domain and from the well known property of the 2D Fourier spectra, which states that the Fourier transform (FT) of a rotated image is the rotated version of the FT applied on the not-rotated image. The idea is to properly define an insertion region in the Cartesian double transformed Fourier domain able to achieve rotation invariance avoiding the need of a log-polar mapping, unlike in (ÓRuanaidh and Pun, 1998) and (Lin et al., 2001). Our approach differs from other methods that embed the mark into the Fourier domain since a single robust feature, extracted in this domain, is used to set up the rotation invariant insertion region. Therefore, starting from the detected invariant direction, the watermark is embedded in a ring region covering the middle frequencies in the Fourier domain using the rule described in (Barni et al., 1998).

In the following we present a detailed description of this method and experimental results that evidence the effectiveness of the direction extraction and the watermark retrieval under several distortions.

2 INVARIANT DIRECTION

The key idea is to characterize the invariant direction as the straight line, passing for $(f_x = 0, f_y = 0)$, along which the function $|I(f_x, f_y)|$ has its maximum cumulated value, where $I(f_x, f_y)$ is the Fourier transform of an image $i(x,y)$. (Heretoafter it is intended that the "zero" frequency location is $(f_x = 0, f_y = 0)$). Hence the invariant direction is uniquely identified by the angle θ_{inv} formed by the extracted line with a reference direction. From the previous definition it can be inferred that the Radon transform (Toft, 1996) is the fundamental tool for the extraction of the invariant feature.

The placement of the invariant direction in the Fourier domain is motivated by two reasons. Since the embedding is performed in the Fourier domain, it is a rationale to extract a synchronization feature in the same domain. Moreover, a watermarked image can undergo attacks modifying either the whole image or circumscribed part of it, hence the Fourier domain has the advantage that local modifications in the spatial domain are always spreaded.

The invariant direction is used as resynchronization feature, which enables the watermarking system to identify the same direction from every distorted $I'(f_x, f_y)$; in this way, whether the image has been rotated by an angle α, the invariant direction $(\theta_{inv} + \alpha)$ is extracted, so that the detector and the message will always be synchronized.

Actually the problem is that the extraction of the invariant direction is performed both at the embedding and detection sides; between the two operations the cover image could have been modified by channel distortions (which includes intentional distortions). In order to make the extraction method as robust as possible, a pre-processing step is then applied to the image to get a spectrum (and so, at least partially, an image) which is as less dependent as possible on these modifications.

2.1 Image Pre-processing

The pre-processing is performed to get a spectrum which is less dependent on the modifications that the image can undergo; its effect is then to provide robustness to the direction extraction method.

To get an image representation invariant to channel modifications, the edge feature is pointed out, since edges generally survive (even if distorted) to several distortions and processings. In Fig. 1 the pre-processing chain scheme is fully depicted.

The tool used for the edge extraction is the cascade of a Gaussian low-pass filtering and a morphological gradient, i.e. a morphological operator revealing sharp luminance transitions. This cascade is quite similar to a Laplacian of a Gaussian filtering, usually adopted for edge extraction, being the Laplacian operator here substituted by the morphological gradient operator (Lee et al., 1987). However differences be-

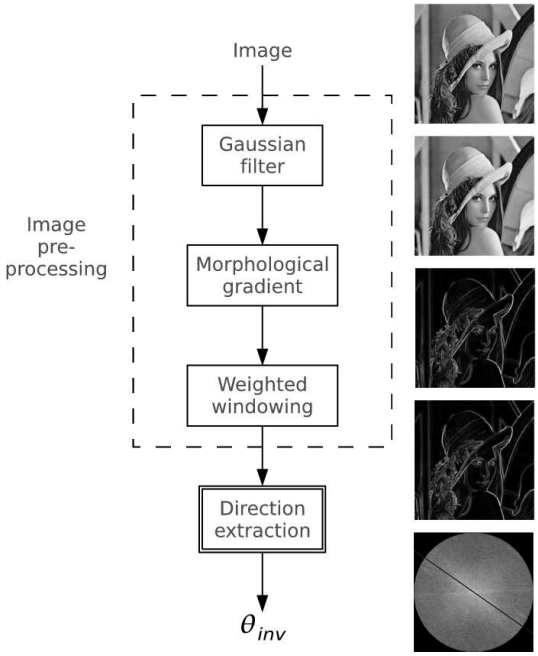

Figure 1: Block diagram of the pre-processing.

tween the twos exist. Laplacian operator associates zero-crossing of second derivatives to an edge, whose location is as close as possible to the real edge (Gonzalez and Woods, 2002), and it is typically followed by a thresholding to convert a gray-scale image into a binary edge image. By the way in this application we are not interested in an accurate location of edges with a binary image but rather in an invariant (and possibly robust against noise) feature extraction through edge enhancement; moreover we are interested to produce edges with thickness as invariant as possible to modifications on image. For this purpose a Gaussian low-pass filtering together with a suitable morphological gradient operator, able to enhance and to widen the edges, can fit as well.

Referring to Fig. 1, the image is firstly low-pass filtered by a Gaussian filter, in order to reduce the higher frequencies energy, which in detection could be due to noise added by the channel; then the morphological gradient of the image is computed. The chosen morphological structuring element has size 5 and has a symmetry as close as possible to a circular one.

The effects on the image spectrum of the morphological operations are not straightforward because of their non-linear nature. An intuitive explanation is that edge sharpening yields an increase of both low frequencies and frequency terms related to edges, hence the global effect is comparable to a contrast enhancement on image spectrum, which is a modification useful for the direction extraction method.

The circular symmetric windowing is performed on the enhanced edge image to reduce aliasing effects in the discrete Fourier domain. In fact the FT and the rotation are operations that do not exactly commute in a discrete domain (Stone, H.S. and Tao, B. and McGuire, M., 1998), so we do not expect a perfect identity between the rotated version of the DFT of the image and the DFT computed from the the rotated image. These differences are due to the skew between the directions along which aliasing takes place and the directions of FT axes. The aliasing effects can be just reduced smoothing the boundaries with a circular and symmetric window (Stone, H.S. and Tao, B. and McGuire, M., 1998). The adopted windowing function has unit value within the circumference of radius $r_1 = (k_1/2)\sqrt{N \cdot M}$ and is zero outside the circumference of radius $r_0 = (k_0/2)\sqrt{N \cdot M}$, with a raised cosine connection in the middle region; N and M are the image dimensions.

In our application, we have chosen empirically the parameters values $k_0 = (4/5)$ and $k_1 = (1/5)$ processing a standard image database.

2.2 Invariant Direction Extraction Method

In the diagram depicted in Fig. 2 the processing chain constituting the invariant direction extraction method is shown. These operations are performed on the pre-processed image as obtained from the processing chain presented in subsection 2.1.

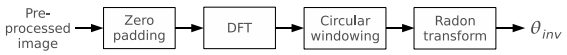

Figure 2: Block diagram of the direction extraction method.

The image is firstly checked to have the same dimensions; if $N \neq M$, the shortest dimension is padded with zeroes to obtain a square matrix before the computing of the DFT.

Invariant direction extraction is performed using the Radon transform on the transformed image. The Radon transform is thus computed over directions passing through the zero frequency:

$$R(0,\varphi)[f(x,y)] = \\ = \int_{-\infty}^{\infty}\int_{-\infty}^{\infty} f(x,y)\,\delta(y - x\tan(\varphi))\,dx\,dy \quad (1)$$

Actually a Discrete Radon transform is computed on the image DFT, using a simple sum approximation. The Radon transform on a finite rectangular domain does not consider that, on different lines, dif-

ferent amounts of pixels lie and consequently diagonals are privileged directions, causing mistaken estimation. The circular windowing before the Discrete Radon Transform can prevent this effect since along every line a fixed amount of non-zero terms lies (Jafari-Khouzani and Soltanian-Zadeh, 2005).

Computing of Radon transform in a discrete context implies that a finite set of direction equally spaced between $[0,\pi[$ must be chosen: $\varphi_i = i \cdot \Delta\varphi$, $i = 0,1,\cdots,(\lfloor \pi/\Delta\varphi \rfloor - 1)$.

Eq. (1) can be rearranged

$$R(0,i)[|I(f_x,f_y)|] = \\ = \Delta f_x \sum_{k=0}^{N-1} |I(k\Delta f_x, \tan(\varphi_i)\, k\Delta f_x)| \quad (2)$$

where Δf_x and $\Delta\varphi$ set the sampled lines along which the cumulated value of Radon transform are computed. Since the Cartesian grid of (f_x, f_y), for which the DFT values are available, will generally not coincide with the grid $(k\Delta f_x, \tan(\varphi_i)\, k\Delta f_x)$, a linear 2D interpolation is used to compute the values of $|I(f_x,f_y)|$ in the needed positions.

After the computing of the discrete Radon transform, the invariant direction angle θ_{inv} will be equal to the φ_i for which

$$\theta_{inv} = \max_{\varphi_i \in [0,\pi[} \{R(0,i)[|I(f_x,f_y)|]\} \quad (3)$$

occurs.

3 EMBEDDING AND DETECTION

The embedding of the message is performed in the Fourier domain using the embedding method described in (Barni et al., 1998). The message is inserted into a sorted subset of the coefficients of the doubly transformed domain, obtained as the intersection of a circular crown region with a finite subset of straight lines belonging to a sheaf:

$$(f_x,f_y)\, t.c. \begin{cases} R_{min} \le ({f_x}^2 + {f_y}^2) \le R_{max} \\ \\ f_y = \tan(\theta_{inv} + i \cdot \Delta\theta) \cdot f_x \\ \qquad\qquad i = 0,\cdots,(\lfloor \pi/\Delta\theta \rfloor - 1) \end{cases} \quad (4)$$

where θ_{inv} is the invariant direction extracted in (3). Thus the detector and the embedder are synchronized, since they consider the straight lines belonging to the sheaf in an ordered sequence starting with the same one, indexed by θ_{inv}. From the previously defined insertion region, an ordered sample sequence is extracted and the mark is inserted into this, according to the chosen rule and according to the symmetry properties of the Fourier transform. For the embedding too, a linear 2D interpolation is needed to get the values of the image in the locations belonging to the above-defined sheaf.

According to (Barni et al., 1998), the message $W = \{w_1,\cdots,w_L\}$ consists of a pseudo-random sequence, each value w_i being a random real number with normal distribution, zero mean and unitary variance. The multiplicative embedding rule is

$$t'_i = t_i + g\, w_i |t_i| \quad (5)$$

where g is a gain factor modulating the embedding strength.

Since the DFT of a real signal is complex valued, the embedding of the same message will be performed twice, both in real and imaginary parts of the DFT samples, taking care to preserve the complex conjugate symmetry of the spectrum.

The detector is built so that, given an image in input, once the invariant direction has been extracted, it can retrieve the marked sample sequence. Then the detector verifies what message has been inserted computing a correlation coefficient between the marked, and possibly corrupted, sample sequence extracted from the image and every codeword belonging to a shared watermark codebook, known both at embedder and at detector sides. The correlation coefficient will be used as measure of the mark presence at the detector.

4 RESULTS

Herein some experimental results are shown, obtained processing standard images, whose size is typically 512x512 pixels.

The effectiveness of the direction extraction method is a needed condition for the decoder and the mark to be synchronized. The following results were obtained computing the Radon transform of the windowed DFT of a pre-processed image along a finite set of directions equally spaced with a step $\Delta\varphi = 0.5\ deg$ and choosing the direction with the maximum cumulated value, as described in section 2.

In Figs. 3(a)–(d) the right working of the proposed direction extraction method is exhibited. In Fig. 3(a) the pre-processed Lena image is depicted while in Fig. 3(b) its windowed spectrum is shown and the extracted invariant direction is highlighted. Rotating by an angle of 30 *deg* the Lena image, we had the pre-processed image and the windowed spectrum depicted respectively in Figs. 3(c) and 3(d). Comparing the highlighted directions in Figs. 3(b) and 3(d), the

rotation of the invariant direction according to the rotation of the original image is noticeable.

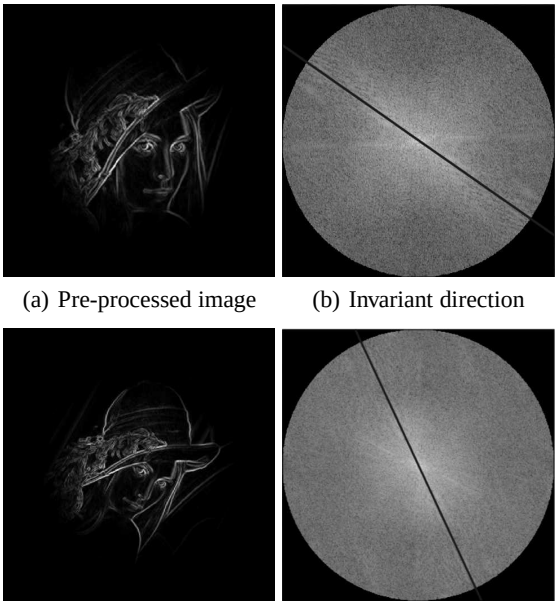

(a) Pre-processed image (b) Invariant direction

(c) Pre-processed rotated image (d) Invariant direction

Figure 3: Example of pre-processing on Lena image with extraction of invariant direction for both original and rotated cases.

In order to measure the effectiveness of the direction extraction method, we compared the extracted invariant directions before and after the embedding and attacks. We tested the algorithm against both common signal processing techniques (Additive White Gaussian Noise, JPEG compression and smoothing) and geometric distortions (rotation, scaling and cropping). Cropping attack was performed cutting away both symmetrically and asymmetrically the framing part of the marked image, but preserving the image center (where the most relevant information is supposed to be located).

The experimental results are listed in Table 1, where $\Delta\theta_{inv} = \theta'_{inv} - (\theta_{inv} + \alpha) mod\ \pi$ is the difference of extracted directions at the detection and embedding sides. The angle values are expressed in *deg*, while the results for cropping attacks are indexed by the percentage of pixels constituting the cropped image with respect to the original one.

Besides, the direction extraction method performs well against random line removal attack too (experimental results here are not shown).

Afterwards some experiments were performed to evaluate the effectiveness of the whole embedding/detection scheme. We embedded a mark sequence of length 9800 samples along 70 directions into the DFT domain and the gain factor in the embedding rule was fixed at the value $g = 1$.

Table 1: Invariant directions extracted from attacked images.

Image		Lena	Peppers	Boat
Invariant direction		145	173.5	113.5
Attack		$\Delta\theta_{inv}$	$\Delta\theta_{inv}$	$\Delta\theta_{inv}$
AWGN	$\sigma = 10$	-0.5	0	0
	$\sigma = 15$	-0.5	0	0
	$\sigma = 20$	0	0	0
JPEG	quality = 50	-0.5	0	0
	quality = 30	0	0	0
	quality = 20	0	0	0
	quality = 10	0	0	0
Smoothing	Average	0	0	0
	Gaussian	0	0	0
	Median	0	0	0
Rotation	$\alpha = 1$	0	0	0
	$\alpha = 5$	-0.5	-0.5	0
	$\alpha = 45$	-0.5	-1	-0.5
	$\alpha = 60$	-0.5	-0.5	-0.5
	$\alpha = 90$	-0.5	0	0.5
	$\alpha = 120$	-0.5	-0.5	0
	$\alpha = 160$	0	-0.5	-0.5
	$\alpha = -1$	0	0	0
	$\alpha = -5$	-0.5	-0.5	0
	$\alpha = -45$	-0.5	-1	-0.5
	$\alpha = -60$	-0.5	-0.5	0
	$\alpha = -90$	-0.5	0	0.5
	$\alpha = -120$	-0.5	-0.5	-0.5
	$\alpha = -160$	0	1	0
Scaling	scale = 0.5	1.5	0.5	0
	scale = .75	1.5	0	0
	scale = 1.5	0	0	0.5
	scale = 2	0	0.5	0
Cropping	rem% = 85	1.5	0	0
	rem% = 78	1.5	0	0
	rem% = 65	-2.5	0	0
	rem% = 53	-2.5	0	0

In order to evaluate the imperceptibility of the watermarking method, the adopted distortion metric is the often used peak to signal noise ratio (PSNR). The PSNR has been computed for the images in database embedding 1000 different watermarks. For the processed images we computed the average PSNR, that resulted to be always greater than 40 dB and its standard deviation which was in the range .1 to .2 dB.

To check the robustness of the whole system, some gray scale standard images were watermarked and both signal processing and geometric attacks were applied to these images. The detector output reveals the estimated embedded message as the one having the greatest correlation coefficient with the sample sequence extracted from the marked and possibly corrupted image. Thus, from the detector re-

sponse to all the codewords belonging to the codebook, we measured the first-to-second peak ratios (P_1/P_2) in decibel.

In the experimental results, listed in Table 2, the index $\tilde{n}$ represents the codeword retrieved from the attacked image by comparison of the correlation coefficients. These results were obtained processing the standard image Boat, but similar results have been obtained with other standard images. Here the results for the cropping attack are related only to symmetrical cuts of the framing part of the marked image, since for asymmetrical cropping the watermark retrieving have shown to fail.

Table 2: Detection results on the attacked image Boat.

Embedded codeword index		$n = 259$	
		Correlation detector	
Attack		$\tilde{n}$	$P_1/P_2(dB)$
AWGN	$\sigma = 10$	259	3.99
	$\sigma = 15$	259	4.61
	$\sigma = 20$	259	4.38
JPEG	QF= 50	259	3.64
	QF= 30	259	3.38
	QF= 20	259	2.61
Smoothing	Average	259	3.35
	Gaussian	259	3.55
	Median	259	3.15
Rotation	$\alpha = 1$	259	3.73
	$\alpha = 5$	259	3.82
	$\alpha = 45$	259	3.69
	$\alpha = 60$	259	2.22
	$\alpha = 90$	259	3.69
	$\alpha = 120$	259	3.75
	$\alpha = 160$	259	1.98
	$\alpha = -1$	259	3.83
	$\alpha = -5$	259	3.56
	$\alpha = -45$	259	4.05
	$\alpha = -60$	259	4.66
	$\alpha = -90$	259	3.69
	$\alpha = -120$	259	4.18
	$\alpha = -160$	259	4.26
Scaling	scale = 0.5	Fail	-
	scale = .75	Fail	-
	scale = 1.5	Fail	-
	scale = 2	Fail	-
Cropping	rem% = 85	259	4.50
	rem% = 78	259	4.08
	rem% = 65	259	3.35
	rem% = 53	259	2.95

By inspection of the results listed in Table 2 it is verified the robustness of the proposed scheme against almost all the tested attacks. In particular the correct mark retrieving is guaranteed even if a slight error in extracted direction occurs. However the watermark recovering fails if the marked image is scaled up or down, though the invariant direction is correctly retrieved (see Table 1). This is due to the inability of the embedding/detection method to cope with the transformed domain enlargement resulted from the image scaling.

5 CONCLUSIONS

In this paper, a watermarking system has been proposed that is robust against both processing and geometric attacks, with particular reference to rotations. A feature extraction method based on Radon transform has been explained; this method is able to retrieve from image spectra a direction that is invariant to geometric transformations on the image. This feature is used to synchronize the detector and the region in the 2D DFT domain wherein the watermark is inserted, guaranteeing the watermark recovering.

Experimental results demonstrate the robustness of both the invariant direction and the watermark embedding against common processing and many of geometric attacks.

Achieving robustness against scaling attacks by an improvement of the embedding method is even possible. Authors are still working in this direction, together with the testing of the robustness after combined attacks.

REFERENCES

Barni, M., Bartolini, F., Cappellini, V., and Piva, A. (1998). A dct-domain system for robust image watermarking. *Signal Process.*, 66(3):357–372.

Bas, P., Chassery, J.-M., and Macq, B. M. (2000). Robust watermarking based on the warping of predefined triangular patterns. In *Proc. SPIE Vol. 3971, Security and Watermarking of Multimedia Contents II*, pages 99–109.

Gonzalez, R. C. and Woods, R. E. (2002). *Digital image processing*. Prentice Hall.

Jafari-Khouzani, K. and Soltanian-Zadeh, H. (June 2005). Rotation-invariant multiresolution texture analysis using radon and wavelet transforms. *Image Processing, IEEE Transactions on*, 14(6):783–795.

Lee, J., Haralick, R., and L.G., S. (1987). Morphological edge detector. *Robotics and Automation, IEEE Transactions on*, 3(2):142–153.

Licks, V. and Jordan, R. (July-Sept. 2005). Geometric attacks on image watermarking systems. *Multimedia, IEEE*, 12(3):68–78.

Lin, C.-Y., Wu, M., Bloom, J., Cox, I., Miller, M., and Lui, Y. (May 2001). Rotation, scale, and translation resilient watermarking for images. *Image Processing, IEEE Transactions on*, 10(5):767–782.

ÓRuanaidh, J. J. and Pun, T. (1998). Rotation, scale and translation invariant spread spectrum digital image watermarking. *Signal Process.*, 66(3):303–317.

Simitopoulos, D., Koutsonanos, D., and Strintzis, M. (2002). Image watermarking resistant to geometric attacks using generalized radon transformations. *Digital Signal Processing, 2002. DSP 2002. 2002 14th International Conference on*, 1:85–88 vol.1.

Stone, H.S. and Tao, B. and McGuire, M. (1998). Analysis of image registration noise due to rotationally dependent aliasing. Technical Report TR 98-018, Nec Research Institute Tech. Rep.

Toft, P. (1996). *The Radon Tranform - Theory and Implementation*. PhD thesis, Department of Mathematical Modelling, Technical University od Denmark.

Xin, Y., Liao, S., and Pawlak, M. (2-5 May 2004). Geometrically robust image watermarking via pseudo-zernike moments. *Electrical and Computer Engineering, 2004. Canadian Conference on*, 2:939–942 Vol.2.